

# The Influence of Temperature on Mode I Fracture Toughness and Fracture Characteristics of Sandstone

Gan Feng<sup>1,3</sup> · Yong Kang<sup>1,4</sup> · Tao Meng<sup>2</sup> · Yao-qing Hu<sup>2</sup> · Xiao-hong Li<sup>1,4</sup>

Received: 26 November 2016 / Accepted: 16 April 2017 / Published online: 25 April 2017  
© Springer-Verlag Wien 2017

**Abstract** This study investigated the influence of temperature on the mode I fracture toughness of sandstone using semicircular bend specimens. Fracture characteristics were studied using scanning electron microscopy and other means. The results showed that temperature influenced fracturing in three stages along a temperature gradient. In the low-temperature stage (20–100 °C), fracture toughness increases slowly, with a total increase of approximately 11%. At the medium-temperature stage (100–500 °C), fracture toughness decreases slowly, at a rate of approximately 18%. During the high-temperature stage (500–800 °C), fracture toughness was reduced by approximately 44%. The mode I fracture toughness has a clear temperature threshold (500–600 °C). Below this threshold, the fracture toughness decreases slowly. When the temperature threshold is reached, the fracture toughness decreases sharply. The sharp decrease is mainly caused by the creation of a fragmentation structure. The sandstone experiences more transgranular fracture mechanics in the low-temperature stage compared to the high-temperature stage. Above 100 °C, the mechanisms include transgranular fracturing, intergranular fracturing, thermal cracking, and mutual coupling fracturing. When the temperature exceeds 500 °C, several different

fragmentation structures are seen. This research study provides significant data to evaluate fracture characteristics and rock safety and stability after heat treatment.

**Keywords** Sandstone · Fracture toughness · Semicircular bend · Fracture crack shape · Fracture analysis

## Abbreviations

SCB	Semicircular bend
SEM	Scanning electron microscopy
ISRM	International Society of Rock Mechanics
$R$	Sample radius (mm)
$B$	Sample thickness (mm)
$a$	Pre-crack length (mm)
$S$	Support span (mm)
$P$	Load (N)
$D$	Sample diameter (mm)
$K_{IC}$	Mode I fracture toughness (MPa mm <sup>1/2</sup> )
$P_{max}$	Peak load of specimen failure (N)
$Y'$	Dimensionless stress intensity factor
UCS	Uniaxial compressive strength (MPa)
$T$	Temperature (°C)
$\sigma_t$	Average UCS (MPa)
$\varepsilon_t$	Average peak strain (10 <sup>-3</sup> )
$E_t$	Average elastic modulus (GPa)
$S_{max}$	Deviation distance (mm)
XRF	X-ray fluorescence
XRD	X-ray diffraction

✉ Yong Kang  
kangyong@whu.edu.cn

<sup>1</sup> Hubei Key Laboratory of Waterjet Theory and New Technology, Wuhan, China

<sup>2</sup> Institute of Mining Technology, Taiyuan University of Technology, Taiyuan, China

<sup>3</sup> School of Civil and Architectural Engineering, Wuhan University, Wuhan, China

<sup>4</sup> School of Power and Mechanical Engineering, Wuhan University, Wuhan, China

## 1 Introduction

Fracture damage is a common phenomenon when rock is exposed to significant temperature differences. Understanding rock fracturing has important applications in

many engineering fields. For example, understanding rock mechanics makes it easier to further develop rock fissures and form better channels through pores and cracks. This can facilitate geothermal extraction from hot dry rock, in situ exploitation of oil–gas from oil shale, and coal bed methane displacement and exploitation using supercritical carbon dioxide injection (Chen and Jiang 2015; Razvigorova et al. 2008; Yang et al. 2012). When exposed to different temperatures, rock breaks intensely, the block size decreases, and the specific surface area increases. This improves the heat energy exchange efficiency and the oil–gas output.

Sometimes, fracturing is desirable; however, controlling that fracturing is important in many underground engineering fields. This includes controlling environments and rock stability near roadways, near mining engineering sites, and near the sealed space of radioactive nuclear waste (Xie et al. 2015; Tsang et al. 2005). During the underground coal gasification process, the stability of surrounding rock is the key factor influencing coal gasification. Because gasification temperatures often reach 1000 °C, high temperatures have a long-term effect on the coal seam roof and floor rock, as the physical and mechanical properties of the rocks are changed. For example, after rocks undergo heat treatment, the elastic modulus, compressive strength, tensile strength, and porosity change (Sirdesai et al. 2016; Sirdesai et al. 2017). These problems are all related to temperature, so studying rock damage and fracturing, especially the physical and mechanical properties of the rock after heat treatment, is of great significance in engineering.

During geological evolution, external forces create many pores and cracks occur in the natural rock. Internal micro-cracks initiate and propagate, and macro-fractures form. These fractures then break (Wong et al. 2001). The fracture toughness reflects the rock's ability to resist crack propagation. Toughness is an important mechanical property index of rock and can be used to characterize the residual strength of rock with crack structures.

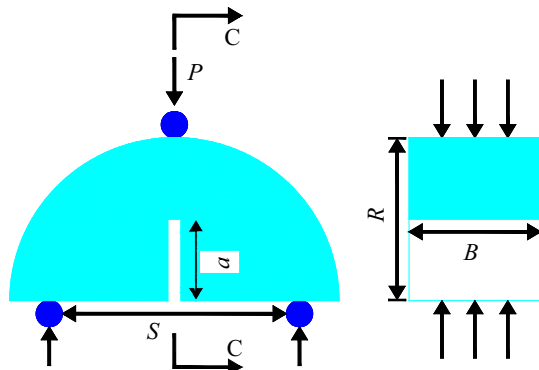
Many researchers have studied the influence of temperature on the fracture toughness of rock. For example, Meredith and Atkinson (1985) used the double-torsion testing method to measure the fracture toughness of granite and gabbro. At temperatures above 100 °C, the fracture toughness decreased, due to the development of micro-cracks caused by uneven thermal expansion between adjacent mineral particles. Research by Zhang et al. (2001) showed that at 20–100 °C, the fracture toughness of gabbro decreased, most likely due to the different structure and rock mineralogy. Al-Shayea (2002) reported that fracture toughness of limestone increased by approximately 25% at 116 °C.

Using straight edge-notched round bar bend (SENRB) specimens and semicircular bend (SCB) specimens,

Funatsu et al. (2004) studied changes in fracture toughness of Kimachi sandstone and Tage tuff. For Kimachi sandstone, the fracture toughness was constant between ambient temperature and 125 °C; fracture toughness increased from 125 to 200 °C, and the fracture toughness increased. These changes were attributed mainly to the drying of the clay material. For Tage tuff, the fracture toughness decreased between room temperature and 75 °C; micro-cracks were the dominant mechanism. From 75 to 200 °C, the fracture toughness increased; this was also attributed to the drying of the clay materials. Balme et al. (2004) observed that fracture toughness increased at temperatures from 100 to 150 °C, due to the closure of micro-cracks caused by thermal expansion. Zuo et al. (2014) found that when the temperature was below 200 °C, fracture toughness increased as the temperature fluctuated, mainly due to temperature induced pore pressure changes; above 200 °C, thermal cracking greatly reduced the fracture toughness. Mahanta et al. (2016) studied the fracture toughness of three kinds of rocks. Fracture toughness increased between ambient temperature and 100 °C; fracture toughness decreased from 100 to 600 °C.

Most current research focuses on conditions with temperatures up to 600 °C; there is a lack of research about the influence of temperature on fracture toughness above 600 °C. There is also a shortage of studies about the change of fracture toughness caused by the change in composition and structure of rock when exposed to heat treatment. In addition, past studies have been designed with relatively short specimen holding times. When the holding time is too short, the rock does not fully reach the intended temperature, and a sufficient reaction time cannot be guaranteed. This study investigated the fracture toughness and fracture characteristics for sandstone, at temperature up to 800 °C.

In fracture mechanics, there are three basic fracture modes: mode I, mode II, and mode III. Mode I fracturing is the most common and most dangerous. The International Society of Rock Mechanics (ISRM) proposed several methods to assess mode I fracture toughness in 1988, 1995, and 2014. Ouchterlony (1988) recommended using the chevron bend (CB) test and short rod (SR) test; ISRM (1995) recommended using the cracked chevron-notched Brazilian disk (CCNBD) method; and Kuruppu et al. (2014) recommended using the semicircular bend (SCB) test. Suitable test methods for assessing mode I fracture toughness require specimens with a simple geometry. The sample development process should be economical; and the test procedure should be convenient and easy to operate (Kataoka et al. 2015). The SCB method meets these criteria (shown in Fig. 1) and is one of the best methods to estimate the fracture toughness of rock. As such, this study used the SCB test method to estimate the fracture toughness of sandstone.



*R*-Sample radius; *B*-Sample thickness; *a*-Pre-crack length *S*-Support span; *P*-Load

**Fig. 1** SCB specimen geometry and schematic loading arrangement

## 2 Specimen Preparation

The test specimen for this study was sandstone, collected from a coal seam roof in the Datong Mining Area of China. The sandstone's density was  $2.65 \text{ g cm}^{-3}$ ; the uniaxial compressive strength was 33 MPa; and the uniaxial tensile strength was 5.0 MPa. Table 1 summarizes the specimen parameters, based on the ISRM-recommended standard specimen size ranges (Kuruppu et al. 2014).

The drill rock core was processed into a disk specimen with a diameter of 50 mm and a thickness of 20 mm. The cutting blade thickness resulted in a significant reduction in sample size; as such, a disk was cut into a half disk. The vertical line lay at the center of the semicircle axis. The length of the artificial pre-crack was 12.5 mm, and the pre-crack width was less than 2 mm. Figures 2 and 3 show the specimen processing process.

## 3 Fracture Toughness Test

### 3.1 Test Contents and Steps

1. Experimental tests were conducted at nine different temperatures, at increasing increments of  $100^\circ$ . The temperatures included: ambient temperature ( $20^\circ\text{C}$ ), 100, 200, 300, 400, 500, 600, 700, and  $800^\circ\text{C}$ .

**Table 1** ISRM-recommended geometrical dimensions of SCB specimen

Descriptions	Values or range
Diameter ( <i>D</i> )	Larger of $10 \times$ grain size or 76 mm
Thickness ( <i>B</i> )	30 mm or larger of $0.4 D$
Pre-crack length ( <i>a</i> )	$0.4 \leq a/R \leq 0.6$
Span length ( <i>S</i> )	$0.5 \leq S/2R \leq 0.8$



(a) Rock drilling machine

(b) Micro milling

**Fig. 2** SCB specimen processing instruments



**Fig. 3** SCB specimen

2. Each SCB specimen was placed in an intelligent heating muffle furnace. These samples were heated slowly, at a constant rate of temperature increase of  $5^\circ\text{C min}^{-1}$ . After the designated temperature was reached, it was held at that level for 10 h, to ensure the internal energy of the specimen reached the preset temperature. This allowed sufficient reaction time. Heating was then stopped, and the specimen was cooled back down to room temperature in the muffle furnace.
3. Each specimen was processed by cutting it artificially. Each specimen was then measured to record the sample thickness and the length of the pre-crack.
4. The fracture toughness test of all SCB specimens was carried out using a Instron material testing machine at the biomechanical testing center of Taiyuan University of Technology in China.

### 3.2 Fracture Toughness Test

This experiment adopted a displacement loading mode, with a loading rate of  $0.0002 \text{ mm s}^{-1}$ . Once preparations were complete, the fracture toughness test was started. A computer recorded the test results. Figure 4 shows the loading mode and the equipment.



Fig. 4 Experimental setup system for the SCB test

### 3.3 Calculation Formula

Experimental data were calculated using the method proposed by ISRM. The fracture toughness  $K_{IC}$  of SCB specimens was calculated using the following formula (Kuruppu et al. 2014):

$$K_{IC} = \frac{P_{\max} \sqrt{\pi a}}{2RB} Y' \quad (1)$$

$$Y' = -1.297 + 9.516(S/2R) - (0.47 + 16.457(S/2R))\beta + (1.071 + 34.401(S/2R))\beta^2 \quad (2)$$

$$\beta = a/R \quad (3)$$

In these expressions,  $P_{\max}$  is the peak load of specimen failure, and  $Y'$  is the dimensionless stress intensity factor. The size for this study was:  $S/(2R) = 0.61$ ,  $a/R = 0.5$ .

## 4 The Results of Fracture Toughness and Loading Curve

### 4.1 The Results of Fracture Toughness

Figure 5 shows the results of the fracture toughness test for the different sandstone specimens at the different temperature levels, using the fracture toughness calculation formula.

As Fig. 5 shows, as the temperature increased from 20 to 800 °C, the average fracture toughness of the specimens changed as follows: 31.46 (20 °C), 34.91 (100 °C), 30.56 (200 °C), 30.46 (300 °C), 27.41 (400 °C), 28.49 (500 °C), 15.43 (600 °C), 15.52 (700 °C), and 16.07 MPa mm<sup>1/2</sup> (800 °C). Between room temperature and 500 °C, the fracture toughness ranged from 27 to 35 MPa mm<sup>1/2</sup>; this

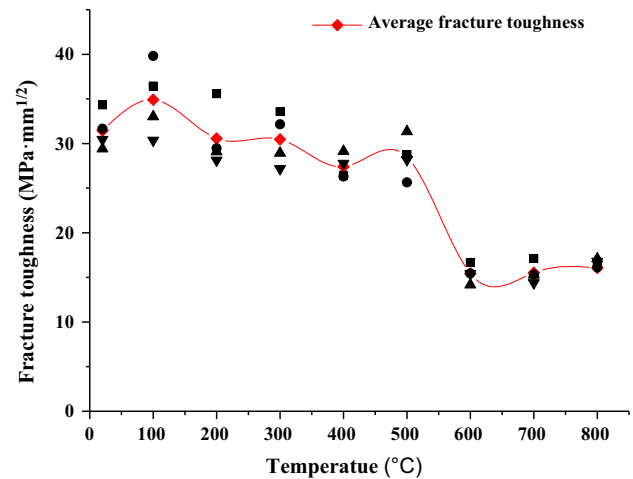


Fig. 5 Fracture toughness at different temperatures

does not reflect a significant change; and the level remained relatively high. Fracture toughness was highest at 100 °C. Compared to ambient temperature, the toughness increased by 10.97% between 20 and 100 °C; the result shows that the temperature increase of 100 °C has the effect of toughening; at 100 °C, the rock's resistance to fracture is the most powerful.

At 400 °C, the fracture toughness reaches 27.41 MPa mm<sup>1/2</sup>, which is the lowest toughness value below 500 °C. At this temperature, the toughness is reduced by approximately 13% compared to ambient temperature. This indicates that the toughness-decreasing effect experiences a significant change at 400 °C; above this, the rock has difficulty resisting fracturing.

When the temperature exceeds 500 °C, the fracture toughness is suddenly reduced from 28.49 MPa mm<sup>1/2</sup> at 500 °C to 15.43 MPa mm<sup>1/2</sup> at 600 °C. This is a reduction of approximately 46%, and reflects the lowest value.

As the temperature continues to increase into the 600–800 °C range, the fracture toughness remains low, but there is little change within this range. Compared to ambient temperature, the toughness decreased by 50.95, 50.67, and 48.92%, at 600, 700, and 800 °C, respectively.

These results indicate that high temperature has a significant toughness-decreasing effect; the rock's ability to resist fracture at high temperatures is greatly weakened. There is a temperature threshold between 500 and 600 °C. When the temperature is below the temperature threshold, the fracture toughness decreases slowly. Once the threshold is reached; fracture toughness is greatly reduced. The fracture toughness is lowest at 600 °C; the rock has the lowest ability to resist fracturing at this point. Therefore, 600 °C is the temperature with the best toughness-decreasing effect.

## 4.2 Load–Displacement Curve

The load–displacement curve was directly obtained using a fracture toughness test. The load–displacement curves of all sandstone specimens were reviewed, revealing similar distribution shapes. Figure 6 provides partial load–displacement curves for each temperature.

Figure 6 shows that these samples are primarily at the linear deformation stage. After the elastic stage, the rock suddenly breaks in a typical brittle failure. Most of the load conditions are in an elastic state before the rock fractures. This further confirms the reasonableness of generally treating rock as elastic.

## 4.3 Uniaxial Compression Test of Sandstone

Fracture toughness of rock is driven by factors in the surrounding environment, such as temperature, humidity, confining pressure, and loading rate. Toughness is also influenced by the physical and mechanical properties of the rock itself, such as fracture toughness and tensile strength, which are correlated (Zhang 2002). Strength is the basic property of sandstone. Therefore, after the same heat

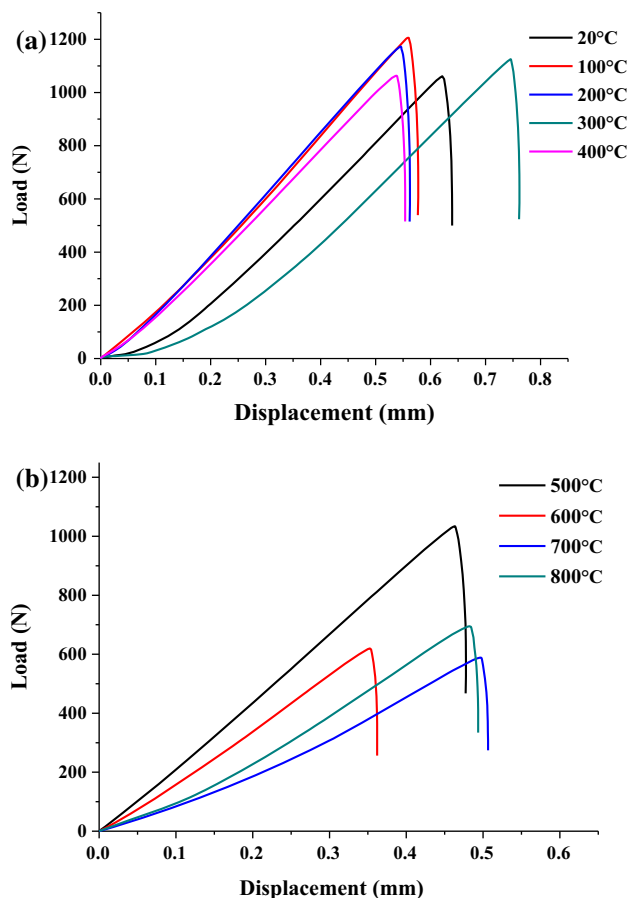


**Fig. 6** Load–displacement curves of sandstone (a, b)

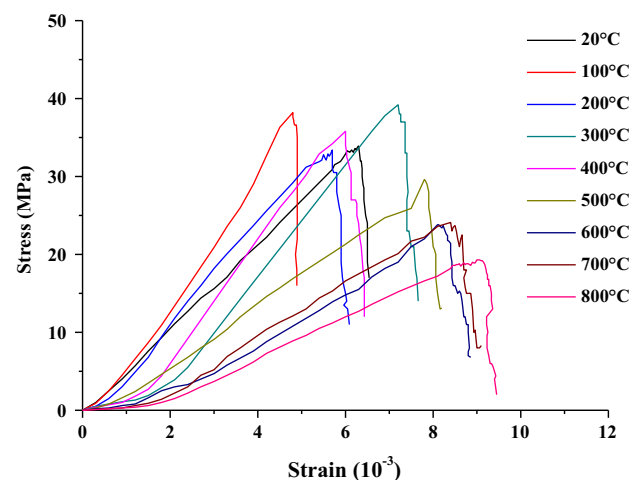
treatment, the standard sandstone samples ( $50 \times 100$  mm) were subjected to an uniaxial compression test. Uniaxial compressive strength is carried out on a WAW-600 microcomputer control electrohydraulic servo universal testing machine. The displacement rate is  $0.0005 \text{ mm s}^{-1}$ . Figure 7 shows the stress–strain curve.

In the uniaxial compression test, the peak stress at the time of rock specimen failure is uniaxial compressive strength (UCS). When the sandstone reaches the peak stress, the corresponding strain is the peak strain. The elastic modulus characterizes the ability of the rock to resist deformation. Table 2 provides the average values of the specimen properties.  $T$  is the temperature;  $\sigma_t$  is the average UCS;  $\varepsilon_t$  is the average peak strain; and  $E_t$  is the average elastic modulus. Figures 8, 9, and 10 show the corresponding curves.

Figure 8 shows that at a temperature below  $500^\circ\text{C}$ , the UCS of the sandstone is between 32 and 39 MPa, with little fluctuation. At  $600^\circ\text{C}$ , the UCS suddenly decreases to 20.6 MPa, a decrease of approximately 37%, significantly reducing sandstone strength. Strength and fracture toughness of rocks are directly proportional to each other (Mahanta et al. 2016). As such, the change of strength generally aligns with fracture toughness trends.

Figure 9 shows that from 20 to  $100^\circ\text{C}$ , the peak strain of sandstone decreased as the temperature increased. At  $100^\circ\text{C}$ , the peak strain is the lowest, at  $6.6 \times 10^{-3}$ . From 100 to  $400^\circ\text{C}$ , the peak strain of sandstone increased slowly, increasing approximately 17%. From 400 to  $800^\circ\text{C}$ , the peak strain of sandstone increased stepwise, reaching a maximum of  $12.2 \times 10^{-3}$  at  $700^\circ\text{C}$ . The high temperature generally increases the sandstone's peak strain.

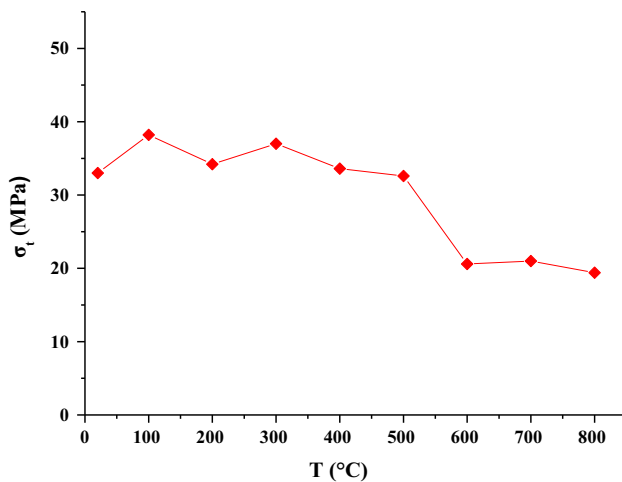
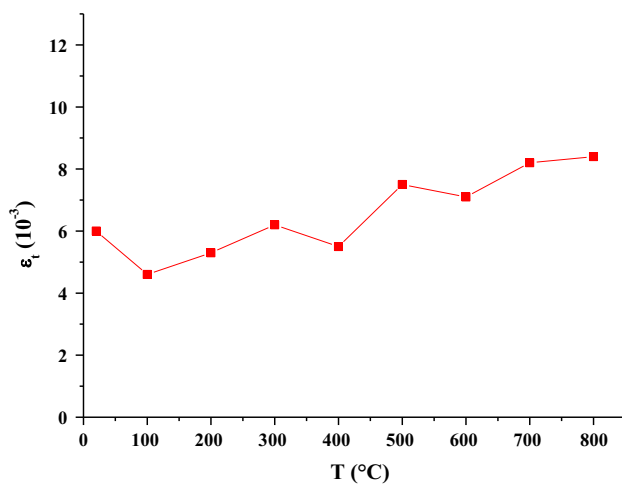
Figure 10 shows that below  $500^\circ\text{C}$ , the elastic modulus of sandstone fluctuated between 5.82 and 7.63 GPa. When



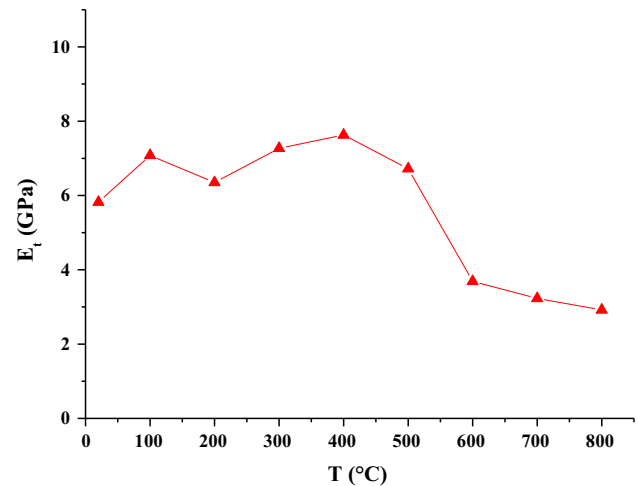
**Fig. 7** Axial stress–strain curves of sandstone after different heat treatments

**Table 2** Sandstone property parameters

$T$ (°C)	$\sigma_t$ (MPa)	$\varepsilon_t$ ( $10^{-3}$ )	$E_t$ (GPa)
20	33	6	5.82
100	38.2	4.6	7.08
200	34.2	5.3	6.35
300	37	6.2	7.27
400	33.6	5.5	7.63
500	32.8	7.5	6.72
600	20.6	7.1	3.69
700	21	8.2	3.23
800	19.4	8.4	2.92

**Fig. 8** UCS versus temperature curve**Fig. 9** Peak strain versus temperature curve

the temperature exceeded 500 °C, the elastic modulus was between 2.92 and 6.69 GPa. The smaller the elastic modulus, the less the sandstone can resist deformation, and the more prone to deformation it is.

**Fig. 10** Elastic modulus versus temperature curve

The UCS curve of sandstone is roughly similar to the elastic modulus curve. Below 500 °C, the sandstone maintained high strength and resist deformation. Once 500 °C was exceeded, the high temperature has a significant effect: the strength decreased, and the sandstone was easily damaged.

## 5 Fracture Characteristics

### 5.1 Fracture Analysis

After the heat treatment, damage created by external forces was assessed by analyzing the properties of the fracture, including fracture morphology and rock mesoscopic features. This analysis can help determine the effect of temperature on the mesoscopic fracturing of sandstone and reveal the effect of temperature on the fracture toughness of sandstone. Fracture morphology analysis using scanning electron microscope (SEM) can help reveal microscopic characteristics and fracture modes of rock (Zangerl et al. 2006). Figure 11 shows the SEM images of the fractured surface of the sandstone.

The formation of cracks within the mineral grain is called transgranular cracks. The formation of cracks around the grain boundaries is called intergranular cracks (Sirdesai et al. 2016). Figure 11b shows typical transgranular and intergranular cracks. The roughness of the fracture surface depends on the fracture modes or failure mechanics. Transgranular fractures are seen in flatter surfaces or surfaces that are less rough, because of higher energy absorption during the fracture process (Mahanta et al. 2017; Liang et al. 2015; Zhang and Zhao 2013; Mecholsky and Mackin 1988).

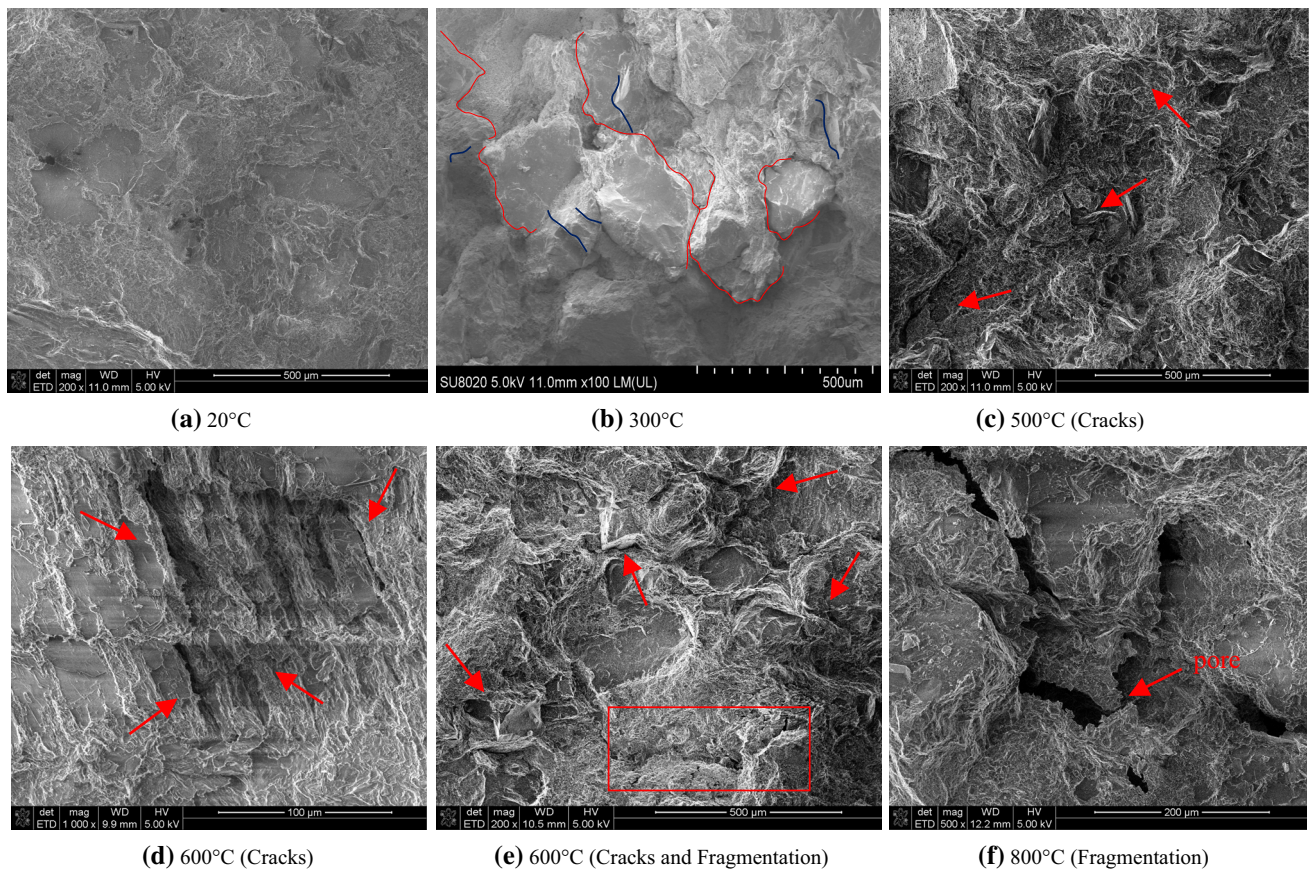


**Fig. 11** SEM images of sandstone; **b** the *red lines* indicate intergranular fracture, and the *blue lines* indicate transgranular fracture. **e** the *box* is the fragmentation structure. **f** is the enlarged graph of fragmentation structure at temperature of 800 °C (color figure online)

The SEM results shown in Fig. 11a indicate that micro-cracks are almost invisible at room temperature. This is because of the weaker effect at lower temperatures. When encountering an external load, the tensile stress generated inside the rock forms transgranular and intergranular fractures. The strength of quartz and feldspar is higher than cement and cuttings; as such, intergranular fractures occurred between the weakly connected particles. Intergranular fractures of the particles themselves also occurred. Due to the high strength of the sandstone at low temperature, the specimen is broken under a large external load. In that case, the fracture path had a less rough fracture surface when compared to the higher temperature heat treatment. Therefore, there were significantly more transgranular fractures at low temperatures.

When the temperature exceeded 100 °C, the thermal effect gradually became more significant; cracks produced by thermal cracking appear after cooling. Secondary cracks formed on the fracture's surface, indicating that fracturing may occur simultaneously in several directions during the formation of the main crack, as shown in Fig. 11c. SEM images for specimens exposed to temperatures of 100–500 °C showed transgranular and intergranular

fractures, thermal cracking, and a coupling fracture mode formed by interactions between fractures. The fracture surface also became increasingly cluttered as the temperature increased, indicating that plastic deformation occurred.

Above 500 °C, the impact of high temperatures on sandstone deterioration appeared more significant. Figure 11d–f shows a messy fracture surface, with increased plastic deformation, and fractures with many cracks, pores, and a wider distribution. Small cracks in the same direction also coalesce, forming a larger cavity. This occurs because the medium grain sandstone is generally porous; particles are not very close to one another; and there are more pores, micro-cracks, and layers. The increased temperature favors pore development. Therefore, the particles are seriously deformed; the particles are disconnected from each other; and the structure deteriorated to form large cracks and pores. Cracks and the accumulation of pore groups transform the rock from a complete structure into a fragmented structure, as shown in Fig. 11e, f. SEM images show that as the temperature increases, the fracture modes of rocks are also more diversified, with clearly visible transgranular and intergranular fractures, thermal ruptures, structural fragmentation degradation, and mutual coupling fractures.

## 5.2 Fracture Crack Shape Analysis

The rock's fracture crack shape is determined by microscopic fracture mechanisms; these shapes can directly reflect the fracture characteristics of rocks. Microscopic fractures reflect rock damage, at the same time, these fractures also provide evidence that explains the rock's ability to resist fracture. Figure 12 shows the crack morphology revealed by observing fracture crack shapes across all cracked specimens on the front and back.

Figure 13 shows the geometrical trajectory of the fracture crack. The middle axis is the direction line of the artificial pre-crack (called the axial direction), and the left and right crack traces are the front and back cracks of the specimen, respectively.

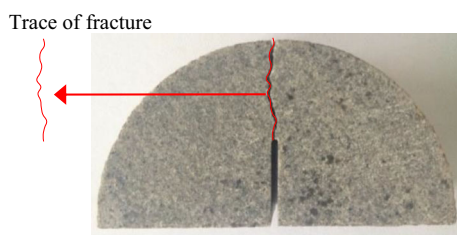


**Fig. 12** Draw traces of fracture

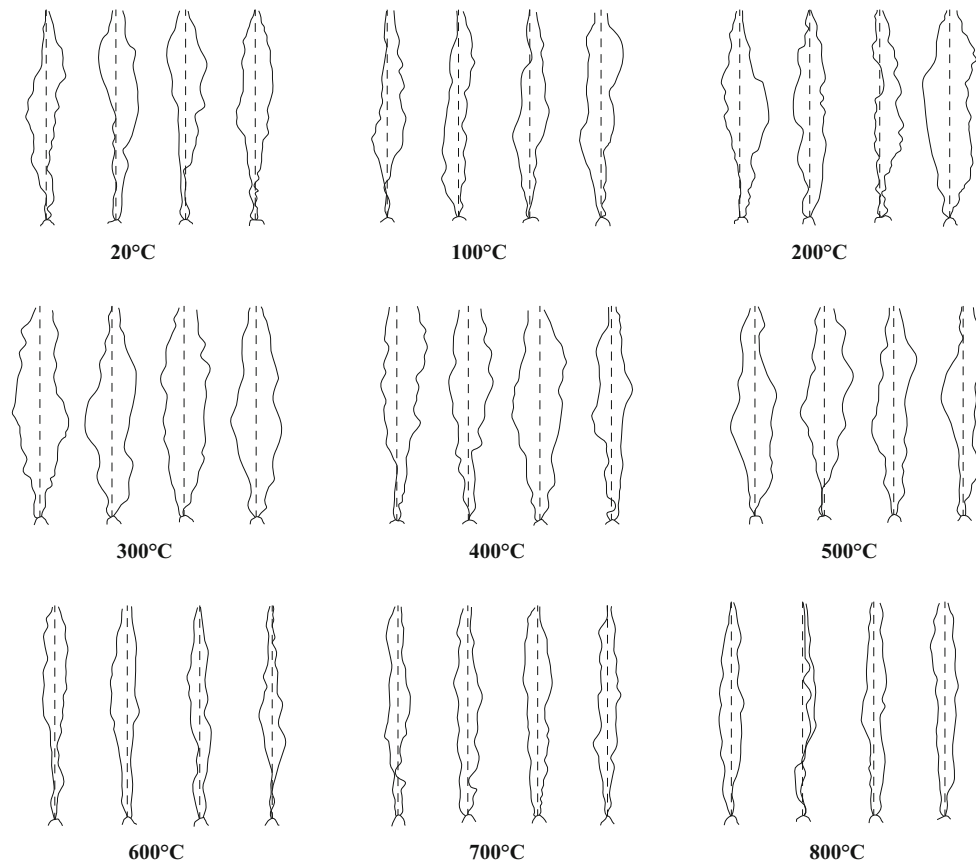


**Fig. 13** Traces of fractures observed on the specimen surfaces of sandstone

The maximum deviation distance was measured to assess the degree of fracture deviation, as shown in Fig. 14.

Table 3 provides the calculated average maximum deviation distance at each temperature.  $T$  represents temperature, and  $S_{\max}$  represents the deviation distance.

These data show that the deviation distance below 500 °C is larger, and the deviation distance above 500 °C is smaller. Sandstone is a brittle material, so tensile properties are weak. Under the external load, the part of the rock with the most tensile stresses is also the part most prone to fracture. A theoretical study by Cotterell and Rice (1980) showed that when considering the fracture crack associated with mode I fracture toughness, the extension stability of the fracture trace depends on the tensile stress. When the tensile stress is negative, the crack propagates along its initial direction. When the tensile stress is positive, the crack propagates away from the initial direction of expansion.

The degree of crack deviation mainly relates to particle size distribution (Kataoka et al. 2015). Particle distribution and internal structure directly impact the fracture mechanism. The temperature weakens the sandstone's internal structure. As the temperature increases from an initially low level, the strength of the mineral particles increases and the connection between particles increases. Tensile



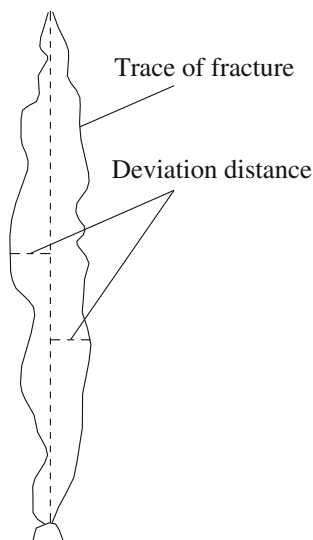


Fig. 14 Deviation distance of fracture

Table 3 Average deviation distance of fracture

$T$ (°C)	$S_{max}$ (mm)	$T$	$S_{max}$ (mm)
20	1.21	500 °C	1.44
100	1.07	600 °C	0.86
200	1.23	700 °C	0.83
300	1.52	800 °C	0.88
400	1.38	–	–

stress is generated in the relatively weak regions between and in the particles. As such, the tensile stress is equally concentrated in the axial direction under the external load; the crack deviation distance decreases between 20 and 100 °C. When the temperature exceeds 100 °C, transgranular, intergranular, and thermal fracturing increases, as does the mutual coupling fracture mechanism. Heat treatments make the clay and cement softening effect more visible. Tensile stress gradually appears between the particles, increasing the probability of fracture cracks along the grain and increasing the degree of crack deviation. Temperatures above 500 °C intensify the softening of the sandstone, reducing its overall strength. Under the external load, crack is easier to extend along the expected axial direction, making the degree of crack deviation small.

## 6 Discussion

### 6.1 The Main Ingredients and Petrographic Thin Section of Sandstone

The fracture toughness of rock is mainly determined by the rock’s composition and structure. As such, one specific

study goal was to determine the major elements in sandstone using X-ray fluorescence (XRF) testing. The results show that the original sandstone had the highest levels of SiO<sub>2</sub>, with a mean value of 73.964%. This was followed by Al<sub>2</sub>O<sub>3</sub>, present at an average level of 16.831%; there were also small amounts of K<sub>2</sub>O, CaO, Fe<sub>2</sub>O<sub>3</sub>, and P<sub>2</sub>O<sub>5</sub>. The X-ray diffraction (XRD) test was carried out on the sandstone specimens heated at the different temperatures. This was done to test the mineral types and their levels in the sandstone. Figure 15 shows the partial diffraction patterns. The results show that the minerals in the sandstone are mainly quartzite, albite, and rectorite, and a small amount of siderite, calcite, and potassium feldspar.

Different minerals have different thermal expansion coefficients, anisotropies, and other properties. The effects of the high temperatures were not the same; however, carefully comparing the specimen diffraction results revealed that the composition of the sandstone was almost unchanged at 800 °C.

Petrographic thin sections generally reflect the mineral composition and internal structure, helping reveal the mesoscopic characteristics of sandstone. Therefore, the test specimens were transformed into petrographic thin sections, as shown in Fig. 16.

The main sandstone specimens were comprised mainly of quartz (60–65%), cuttings (30–35%), and feldspar (1–5%). Minor components included glauconite, clay hybrids, calcareous cements (2–3%), and dolomitic cements (1–3%). The quartz included mainly monocrytalline quartz, with a common wavy extinction. Feldspar was mainly made of plagioclase and a small amount of potassium feldspar. The size of the mineral particles generally ranged from 200 to 500 μm; cement particles were mainly 1–50 μm. The sandstone was medium grain detritus sandstone, with a medium grain sandy structure. At

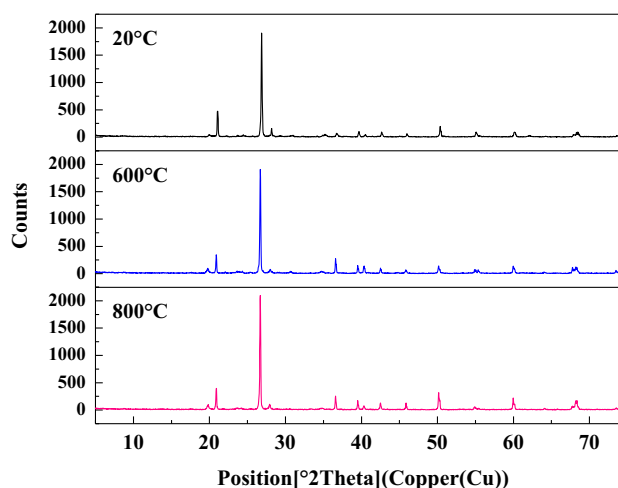
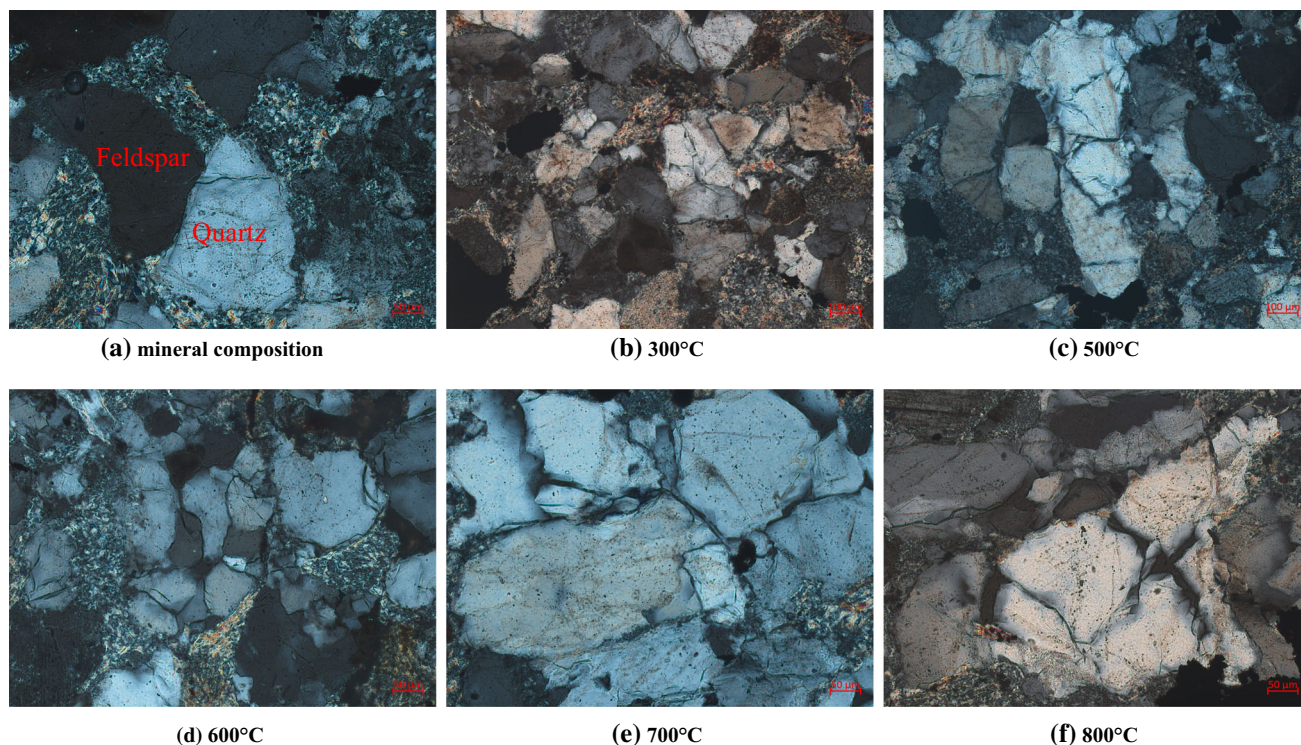


Fig. 15 X-ray diffraction spectrum



**Fig. 16** Petrographic thin sections of sandstone

ambient temperature, there was a small amount of cracking. Figure 16b shows a petrographic thin section of the sandstone sample at 300 °C. It shows a small number of cracks, including both transgranular and intergranular fracture cracks. Figure 16c shows a sample petrographic thin section of sandstone at 500 °C. There are significantly more cracks compared to the thin section at 300 °C. Figure 16d–f shows the thin sections at 600–800 °C. Several transgranular and intergranular fracture cracks and a mutual coupling fracture crack can be seen.

## 6.2 Fracture Toughness and Fracture Characteristic Analysis

Heat treatments can either improve or degrade the physical and mechanical properties of rock. As the rock composition and the external environment change, the dominant mechanism associated with different heat treatments differs. These cause differences in fracture toughness. For example, above 100 °C, evaporation of interlayer and adsorbed water can lead to clay hardening, increasing the fracture toughness of rock (Funatsu et al. 2014). At a temperature above 200 °C, thermal cracking can reduce mineral particles and clay cohesion, causing the fracture toughness of sandstone to decrease (Zuo et al. 2014). At 100–150 °C, fracture toughness increases, due to micro-cracks closure caused by thermal expansion (Balme et al. 2004). The sandstone samples used in this

study were mainly composed of quartz, feldspar, and cuttings, with small amounts of clay and mica. The volume expansion of quartz and mica is four times that of feldspar when exposed to high temperatures. Rocks mainly composed of quartz, mica, and feldspar experience significant changes as the temperature changes (Tian et al. 2012). The changes in fracture toughness as the temperature changes can be roughly viewed as occurring in three stages: the low-temperature stage (20–100 °C), medium-temperature stage (100–500 °C), and high-temperature stage (500–800 °C).

During the low-temperature stage (20–100 °C), the fracture toughness of the sandstone increases slowly, by approximately 11% overall. As the rock is subjected to heat, water evaporation occurs. In general, the interlayer water within the clay mineral is lost at a temperature range of 80–100 °C (Yilmaz 2011). Based on the principle of effective stress, water evaporation from pores and fissures decreases pore pressure and increases effective stress. This results in rock pellets being pressed and the rock strength being improved. Heating also causes thermal stress inside the rock, causing thermal cracking damage. A previous study found that the thermal damage caused by the heat is not reversed after cooling (Gautam et al. 2015). However, the SEM results and petrographic thin section analysis revealed that the specimen heated to 100 °C did not experience significant cracks; little thermal cracking occurs at the low-temperature stage. This is because at this lower

temperature, the thermal stress between the particles and internal mineral granules is not significant enough, so it only causes recoverable elastic deformation (i.e., thermal expansion), and small thermal cracking does not occur. The thermal expansion can cause existing micro-cracks to close, or the thermal expansion can constrain the connection between the existing cracks. This leads to improvements in the overall structural strength of the sandstone.

In addition, the petrographic analysis (Fig. 16) showed that the sandstone contained a small amount of clay and cement. The temperature increase caused the clay to expand, fill, and squeeze internal defects. This increases the overall density, which increases rock strength. The increased rock strength leads to increase resistance to breakage through and along the particles. Given this, the fracture is characterized by a transgranular fracture mechanism and an increase in fracture toughness. The transgranular fracture will inevitably produce macroscopic fracture cracks, with minor deviations from the axis direction. The more transgranular fractures there are, the smaller the deviation. At low temperatures, water evaporation and thermal expansion suppress micro-cracks, increasing fracture toughness. Fracture toughness increases slowly because of the low-temperature effect.

In the medium-temperature range (100–500 °C), the fracture toughness of the sandstone decreases slowly as the temperature increases. At 500 °C, the toughness is approximately 18% lower than at 100 °C and approximately 9% lower than at 20 °C. As the temperature gradually increased, water evaporation became more marked within the rock. There was both full evaporation of the interlayer water and structural water loss. These caused rock dehydration, and it affects rock structure. For example, the serpentine dehydration process produces mode I tensile cracks (Jung et al. 2004). At the same time, water evaporation leads to gradual internal drying of the sandstone, increasing the friction coefficient of mineral particles (Tian et al. 2012). However, the clay and cement content of this sample is very small, so water evaporation has minimal influence. In contrast, the fracture surface and sandstone do have a certain number of internal cracks, and this shows that thermal cracking does occur at this stage, as shown in Figs. 11b, c and 16c, d. This is due to the rise in temperature, causing the thermal expansion coefficient of rock particles to change. The mineral particles thus exhibit an uncoordinated and irreversible thermal expansion (Wong and Brace 1979). Thermal expansion produces thermal stress; when the thermal stress exceeds the surrounding mineral bearing capacity, thermal cracking occurs. The degree of thermal cracking depends mainly on the temperature gradient, with other factors being less significant (Zhao et al. 2008). The higher the temperature goes, the more levels the temperature will increase through

before dropping. This leads to a higher probability of thermal cracking and reduced fracture toughness.

SEM and petrographic analysis indicates that thermal cracking will occur both inside and between the particles. However, the clay and cement heat softening effect is more significant, and the probability of thermal cracking occurring between mineral particles and other particles is increased, increasing intergranular fracturing. The grain size of medium grain sandstone is relatively large, so the intergranular fracture will inevitably produce macroscopic fracture cracks, which deviate more from the axis direction. The more intergranular fractures there are, the greater the degree of crack deviation. SEM results also show that the fracture mechanism of sandstone is intergranular fracturing, transgranular fracturing, thermal fracturing, and a coupling mechanism. This is a more diversified set of actions than fractures that occur at low temperatures. In the medium-temperature stage (100–500 °C), cracks are primarily produced by thermal cracking, decreasing the fracture toughness of sandstone. At 400–500 °C, the fracture toughness increased, with a toughness that was approximately 4% higher than at 400 °C. The weak increase may be caused by the isomerization of sandstone.

In the high-temperature stage (500–800 °C), the fracture toughness decreased by 46%, particularly in the 500–600 °C range. This was the maximum drop, signaling that this stage is the threshold temperature range. The change in fracture toughness was not significant between 600 and 800 °C. This may be due to mineral phase transformation, isomeric recrystallization (Yin et al. 2012), and chemical bond fracturing in minerals such as Al–O, K–O, and Na–O at this high temperature. Further, at this temperature range, some of the minerals in the sample melted, generating several microscopic defects in the rock.

The transformation temperature of the  $\alpha$ – $\beta$  phase transition of quartz is 573 °C. The quartz  $\alpha$ – $\beta$  phase transformation is accompanied by a change in volume, deteriorating the rock's mechanical properties. Quartz makes up to 65% of the sandstone used in this study. The large proportion of quartz increases the uneven expansion of quartz and surrounding minerals, resulting in increasing micro-cracks. An excessively high temperature intensifies the thermal cracking, increases defects, and causes internal structural changes in the rock. The SEM and petrographic thin section results show a significant increase in the number of cracks, as shown in Figs. 11d–f and 16e, f.

The structural changes are seen in the increase and development of porosity and fracturing, which result in reduced particle connectivity, dislocation, and loose areas between the particles. This is particularly true in areas where the pores and fractures converge. This leads to further loosening or a larger direct damage zone, eventually resulting in a fragmentation structure, as shown in Fig. 11e,

f. Such a fragmentation structure greatly reduces the physical properties of sandstone, resulting in the rapid deterioration of the rock's mechanical properties. Component identification reveals that the sandstone composition remains unchanged, even at 800 °C. At the high-temperature range, the fundamental reason for the abrupt decrease in the sandstone's fracture toughness is the generation of the fragmentation structure. The deepening of thermal damage leads to the softening of mineral particles, cements, and clay. The fracture surface is then further weakened, reducing the resistance to transgranular fractures along the axial direction. This leads to a complicated fracture mechanism (intergranular fracturing, transgranular fracturing, thermal fracturing, structural fragmentation, and mutual coupling fracture mechanism) in the sandstone. It also causes the degree of macroscopic crack deviation to decrease under external loads. However, at 600–800 °C, the change in fracture toughness is not significant. This may be because at the excessive temperature levels, the different mechanisms tend to balance one another.

## 7 Conclusions

Using SCB tests and experiments, this study examined the fracture toughness and fracture characteristics of Datong sandstone when exposed to heat treatments at levels between 20 and 800 °C. Key conclusions are as follows.

1. The fracture toughness of sandstone does not experience a singular consistent increase or decrease as the temperatures increase. Instead, there are three stages: the low-temperature stage (20–100 °C) during which the fracture toughness slowly increases; the medium-temperature stage (100–500 °C), during which the fracture toughness slowly drops; and the high-temperature stage (500–800 °C), during which the fracture toughness decreased significantly. At a temperature of 100 °C, there is a clear toughness-increasing effect. Between 20 and 500 °C, 400 °C is the best temperature point to achieve the best toughness-decreasing effect. The toughness-decreasing effect is optimal at 600 °C.
2. The fracture toughness of the sandstone has a clear temperature threshold (500–600 °C). The fracture toughness decreases slowly before the threshold was reached; once the threshold was crossed, the fracture toughness sharply decreased. The threshold temperature range indicates a fundamental change in the fracture toughness of the sandstone and may serve as an important index for engineering projects to evaluate the stability and safety of the rock.
3. There were more transgranular fracture mechanics associated with the sandstone below 100 °C compared to the high-temperature stage. Above 100 °C, the fracturing mechanisms included intergranular fractures, transgranular fractures, thermal fractures, and mutual coupling fractures. At the highest temperatures above 500 °C, there were a large number of fragmentation structures.
4. Between 100 and 500 °C, the degree of deviation of the fracture crack increases as the temperature increases. At temperatures above 500 °C, the fracture crack's degree of deviation decreases.
5. At 20–100 °C, the fracture toughness of sandstone increased slowly, mainly due to water evaporation and micro-crack closure. At 100–500 °C, the fracture toughness of sandstone decreased, mainly due to the development and connection of hot cracks induced by thermal cracking. At 500–800 °C, the fracture toughness of sandstone was greatly reduced, mainly because of the fragmentation structure caused by quartz  $\alpha$ - $\beta$  phase transformation and thermal cracking. The main reason for the abrupt decrease in fracture toughness is fragmentation fracture.
6. The temperature significantly impacts the mechanical properties of sandstone, such as peak load, peak displacement, and equivalent elastic modulus. The changes in equivalent elastic modulus, peak load, and fracture toughness are similar. However, the peak displacement did not follow clear explicit rules.

**Acknowledgements** This study was supported by the National Key Basic Research Development Program of China (973 Program) (Grant No. 2014CB239200) and the National Natural Science Foundation of China (Grant No. 51574173).

## References

- Al-Shayea N (2002) Comparing reservoir and outcrop specimens for mixed mode I–II fracture toughness of a limestone rock formation at various conditions. *Rock Mech Rock Eng* 35(4):271–297
- Balme MR, Rocchi V, Jones C, Sammonds PR, Meredith PG, Boon S (2004) Fracture toughness measurements on igneous rocks using a high-pressure, high-temperature rock fracture mechanics cell. *J Volcanol Geoth Res* 132(2–3):159–172
- Chen J, Jiang F (2015) Designing multi-well layout for enhanced geothermal system to better exploit hot dry rock geothermal energy. *Renew Energy* 74(1):37–48
- Cotterell B, Rice JR (1980) Slightly curved or kinked cracks. *Int J Fract* 16(2):155–169
- Funatsu T, Seto M, Shimada H, Matsui K, Kuruppu M (2004) Combined effects of increasing temperature and confining pressure on the fracture toughness of clay bearing rocks. *Int J Rock Mech Min Sci* 41(6):927–938
- Funatsu T, Kuruppu M, Matsui K (2014) Effects of temperature and confining pressure on mixed-mode (I–II) and mode II fracture

- toughness of Kimachi sandstone. *Int J Rock Mech Min Sci* 67(2):1–8
- Gautam PK, Verma AK, Maheshwar S, Singh TN (2015) Thermo-mechanical analysis of different types of sandstone at elevated temperature. *Rock Mech Rock Eng* 49(5):1985–1993
- ISRM Testing Commission (1995) Suggested method for determining mode I fracture toughness using cracked chevron notched Brazilian disc (CCNBD) specimens. *Int J Rock Mech Mining Sci Geomech Abstr* 32(7):57–64
- Jung H, Green II HW, Dobrzynetska LF (2004) Intermediate-depth earthquake faulting by dehydration embrittlement with negative volume change. *Nature* 428(1):545–549
- Kataoka M, Obara Y, Kuruppu M (2015) Estimation of fracture toughness of anisotropic rocks by semi-circular bend (SCB) Tests Under water vapor pressure. *Rock Mech Rock Eng* 48(4):1353–1367
- Kuruppu MD, Obara Y, Ayatollahi MR, Chong KP, Funatsu T (2014) ISRM-suggested method for determining the mode I fracture toughness using semi-circular bend specimen. *Rock Mech Rock Eng* 47(1):267–274
- Liang C, Wu S, Li X, Xin P (2015) Effects of strain rate on fracture characteristics and mesoscopic failure mechanisms of granite. *Int J Rock Mech Min Sci* 76:146–154
- Mahanta B, Singh TN, Ranjith PG (2016) Influence of thermal treatment on mode I fracture toughness of certain Indian rocks. *Eng Geol* 210:103–104
- Mahanta B, Tripathy A, Vishal V, Singh TN, Ranjith PG (2017) Effects of strain rate on fracture toughness and energy release rate of gas shales. *Eng Geol* 218:39–49
- Mecholsky JJ, Mackin TJ (1988) Fractal analysis of fracture in Ocala chert. *J Mater Sci Lett* 7(11):1145–1147
- Meredith PG, Atkinson BK (1985) Fracture toughness and subcritical crack growth during high-temperature tensile deformation of Westerly granite and Black gabbro. *Phys Earth Planet Inter* 39(1):33–51
- Ouchterlony F (1988) Suggested methods for determining the fracture toughness of rock. *Int J Rock Mech Min Sci Geomech Abstr* 25(2):71–96
- Razvigorova M, Budinova T, Petrova B, Tsyntsarski B, Ekinici E, Ferhat MF (2008) Stem pyrolysis of Bulgarian oil shale kerogen. *Oil Shale* 25(1):27–36
- Sirdesai NN, Mahanta B, Singh TN, Ranjith PG (2016) Elastic modulus of thermally treated fine grained sandstone using non-contact laser extensometer. In: International conference on recent advances in rock engineering, pp 105–109
- Sirdesai NN, Singh TN, Ranjith PG, Singh Rajesh (2017) Effect of varied durations of thermal treatment on the tensile strength of red sandstone. *Rock Mech Rock Eng* 50:205–213
- Tian H, Kempka T, Xu N-X, Ziegler M (2012) Physical properties of sandstones after high temperature treatment. *Rock Mech Rock Eng* 45(6):1113–1117
- Tsang C-F, Bernier F, Davies C (2005) Geohydromechanical processes in the excavation damaged zone in crystalline rock, rock salt, and indurate and plastic clays: in the context of radioactive waste disposal. *Int J Rock Mech Min Sci* 42(1):109–125
- Wong T-F, Brace WF (1979) Thermal expansion of rocks: some measurements at high pressure. *Tectonophysics* 57(2–4):95–117
- Wong RHC, Chau KT, Tang CA, Lin P (2001) Analysis of crack coalescence in rock-like materials containing three flaws—part I: experimental approach. *Int J Rock Mech Min Sci* 38(7):909–924
- Xie S, Li E, Li S, Wang J, He C, Yang Y (2015) Surrounding rock control mechanism of deep coal roadways and its application. *Int J Mining Sci Technol* 25(3):429–434
- Yang T, Nie B, Yang D, Zhang R, Zhao C (2012) Experimental research on displacing coal bed methane with supercritical CO<sub>2</sub>. *Saf Sci* 50(4):899–902
- Yilmaz G (2011) The effects of temperature on the characteristics of kaolinite and bentonite. *Sci Res Essays* 6(9):1928–1939
- Yin T, Li X, Xia K, Huang S (2012) Effect of thermal treatment on the dynamic fracture toughness of laurentian granite. *Rock Mech Rock Eng* 45(6):1087–1094
- Zangerl C, Loew S, Eberhardt E (2006) Structure, geometry and formation of brittle discontinuities in anisotropic crystalline rocks of the Central Gotthard Massif, Switzerland. *Ecolgae Geol Helv* 99(2):271–290
- Zhang ZX (2002) An empirical relation between mode I fracture toughness and the tensile strength of rock. *Int J Rock Mech Min Sci* 39(3):401–406
- Zhang QB, Zhao J (2013) Effect of loading rate on fracture toughness and failure micromechanisms in marble. *Eng Fract Mech* 102:288–309
- Zhang ZX, Yu J, Kou SQ, Lindqvist P-A (2001) Effects of high temperatures on dynamic rock fracture. *Int J Rock Mech Min Sci* 38(2):211–225
- Zhao Y-S, Meng Q-R, Kang T, Zhang N, Xi B (2008) Micro-CT experimental technology and meso-investigation on thermal fracturing characteristics of granite. *Chin J Rock Mechan Eng* 27(1):28–34 (in Chinese)
- Zuo J-P, Xie H-P, Dai F, Ju Y (2014) Three-point bending test investigation of the fracture behavior of siltstone after thermal treatment. *Int J Rock Mech Min Sci* 70(9):133–143